

Nanoscale

Accepted Manuscript



This is an *Accepted Manuscript*, which has been through the Royal Society of Chemistry peer review process and has been accepted for publication.

Accepted Manuscripts are published online shortly after acceptance, before technical editing, formatting and proof reading. Using this free service, authors can make their results available to the community, in citable form, before we publish the edited article. We will replace this *Accepted Manuscript* with the edited and formatted *Advance Article* as soon as it is available.

You can find more information about *Accepted Manuscripts* in the [Information for Authors](#).

Please note that technical editing may introduce minor changes to the text and/or graphics, which may alter content. The journal's standard [Terms & Conditions](#) and the [Ethical guidelines](#) still apply. In no event shall the Royal Society of Chemistry be held responsible for any errors or omissions in this *Accepted Manuscript* or any consequences arising from the use of any information it contains.

Magnetically triggered release of molecular cargo from iron oxide nanoparticle loaded microcapsules

Susana Carregal-Romero^{1,2#}, Pablo Guardia^{3#}, Xiang Yu¹, Raimo Hartmann¹, Teresa Pellegrino^{3*}, Wolfgang J. Parak^{1,2*}

¹ *Fachbereich Physik, Philipps Universität Marburg, Marburg, Germany*

² *CIC Biomagune, San Sebastian, Spain*

³ *Nanochemistry, Istituto Italiano di Tecnologia, Genova, Italy*

both authors contributed equally to this work

* *corresponding authors: teresa.pellegrino@iit.it, wolfgang.parak@physik.uni-marburg.de*

Abstract

Photothermal release of cargo molecules has been extensively studied for bio applications. For instance, microcapsules decorated with plasmonic nanoparticles have been widely used in *in vitro* assays. However, some concerns about their suitability for some *in vivo* application cannot be easily overcome, in particular the limited penetration depth of light (even infrared). Magnetic nanoparticles are alternative heat-mediators for local heating, which can be triggered by applying an alternating magnetic field (AMFs). AMFs are much less absorbed by tissue than light and thus can penetrate deeper overcoming the above mentioned limitations. Here we present iron oxide nanocube-modified microcapsules as platform for magnetically triggered molecular release. Layer-by-layer assembled polyelectrolyte microcapsules with 4.6 μm diameter, which had 18 nm diameter iron oxide nanocubes integrated in their walls, were synthesized. The microcapsules were further loaded with an organic fluorescent polymer (Cascade Blue-labelled dextran), which was used as model of a molecular cargo. Through an AMF the magnetic nanoparticles were able to heat their surroundings and destroy the microcapsule walls, leading to a final release of the embedded cargo to the surrounding solution. The cargo release was monitored in solution by measuring the increase in both absorbance and fluorescence signal after the exposure to an AMF. Our results demonstrate that magnetothermal release of encapsulated material is possible by using magnetic nanoparticles with a high heating performance.

Introduction

For the *in vitro* and *in vivo* delivery of functional molecular cargo (such as drugs or enzymes) it is often beneficial to encapsulate the cargo. Encapsulation can be used to protect the cargo from enzymatic degradation,¹ to alter the intracellular distribution of the cargo within cells, as well as the biodistribution within animals,^{2,3} and to control the release of the cargo.^{4,5} Polyelectrolyte capsules fabricated by layer-by-layer (LbL) assembly offers a convenient approach for cargo encapsulation.⁶ Hitherto, this approach has been mainly optimized for *in vitro* assays, whereby a capsule size on the micrometre scale is beneficial.⁷⁻⁹ However, *in vivo* applications, as for instance vaccination, have been also reported.^{10,11} Controlled release from such microcapsules has been demonstrated *in vitro* using a large variety of

different stimuli including pH,¹² redox potential,¹³ enzymatic degradation,¹ ultrasound,¹⁴ microwaves,¹⁵ and photothermal local heating.¹⁶⁻²⁰ For externally triggered release, photothermal heating has shown to be of great interest as it can be remotely controlled.

Photothermal heating, *i.e.* the local generation of heat upon optical resonant excitation of plasmonic nanoparticles (NPs),²¹ has nowadays reached a high level of control and is used in a variety of biological applications.²²⁻²⁴ As example, photothermal therapy preferentially induces apoptosis in cells by local heating (hyperthermia) of the NPs' surrounding.²⁴⁻²⁶ However this is a delicate process since an elevated power dissipation will lead to a high increase of the temperature and thus (above 100 °C) to the formation of bubbles through water evaporation.²⁷ In such a scenario cells would be destroyed by mechanical effects rather than by apoptosis.^{19, 28} It is worthy to underline that intracellular effects triggered by light activation of plasmonic NPs are not exclusively/solely based on heat generation, but also on the generation of reactive oxygen species.²⁹ Finally, photothermal heating has also been used for light-triggered destruction of carrier matrixes in which plasmonic NPs are embedded, which can be used for the release of encapsulated molecules.³⁰ Besides polymer capsules and particles, also liposomes have been used as carrier matrixes,³¹ Such light-triggered release has reached a degree of control that allows for opening of individual capsules inside cells,²⁰ and thus the subsequent *in vitro* release of different molecular cargo inside cells.⁵ However, concerning potential *in vivo* applications, photothermal heating of plasmonic NPs by optical excitation shows a significant drawback due to the strong absorption of light by tissues, slightly reduced in the so-called biological window in the near infrared.^{32, 33} This issue definitively restricts the use of plasmonic NPs for *in vivo* applications.

Besides plasmonic NPs, magnetic NPs are extensively used as heat-mediators for magnetic induced hyperthermia, in which the heat is produced *via* an alternating magnetic field (AMF).³⁴⁻³⁷ Technically both modes of excitation are based on the excitation through an electromagnetic field but at different frequencies. While for optical heating the frequency of the electromagnetic field is in the range of the visible and the infrared (IR), in the case of magnetic NPs the frequency is in the range of the radiofrequencies (RF). Similar to plasmonic NPs, the capability of magnetic NPs to act as heat-mediators^{38, 39} has been exploited for magnetic mediated hyperthermia treatment⁴⁰⁻⁴² as well as for controlled drug delivery.^{43, 44} However, magnetic NPs have been so far less exploited to trigger release from carrier matrixes such as polyelectrolyte capsules.⁴ In this direction permeability changes of the polymeric walls of capsules with embedded magnetic NPs and drug release upon application of an AMF have been already reported.^{45, 46} Besides heat, AMFs can produce mechanical vibration of magnetic nanoparticles and stretching of polymers in close proximity. This non-heating effect has been exploited as well to control enzymatic activity in nanocomposites.⁴⁷ However, the low heating performance shown by magnetic NPs synthesized by conventional methods so far has set limits to the promising concept drug of remotely controlled delivery by magnetothermal heating,⁴⁸ which requires magnetic NPs with a high heating performance. Recent advances in the synthesis of novel magnetic NPs⁴⁹ have resulted in iron oxide nanocubes as efficient heat-mediators for magnetic induced hyperthermia.⁵⁰ Such cubic iron oxide NPs are preferentially prepared in organic solvents, but can be easily transferred to polar solvents,⁵¹ which will further allow for their integration into polyelectrolyte capsules. Owing the high heating capability of these magnetic NPs, they are appealing NPs to be used to trigger release of molecular cargo from polyelectrolyte capsules and other carrier matrixes *via* magnetothermal heating.

Higher heating capability required use of less nanoparticles, as the highly uniform size distribution of the nanocubes warrants that most nanoparticles lie within the required (size-dependent) resonance frequency and thus contribute towards heating. The concept of remotely controlled release of encapsulated molecules *via* magnetothermal heating has been recently demonstrated for liposomes and hybrid capsules containing a fluorescent probe within the lipidic layer of the capsule wall.^{52, 53} While the proof of concept of this concept thus already has been made, for a more general applicability it still needs to be extended to other type of matrixes as well as improved nanoparticles, which is the objective of this report.

Here we present a proof of concept of magnetic triggered release of a model molecule using polyelectrolyte microcapsules as carrier matrix. Polyelectrolyte microcapsules bearing iron oxide nanocubes as magnetic NPs in their walls were loaded with Cascade Blue-labelled dextran and the latter released by applying an AMF.

Materials and Methods

Magnetic nanoparticles synthesis: Synthesis of water-soluble iron oxide nanocubes with core size of 18 ± 2 nm were synthesized according to a previously published protocol.⁵¹ Iron (III) acetylacetonate (99%), decanoic acid (99%) and dibenzyl ether (99%) were purchased from Acros. Squalane (98%) was purchased from Alfa Aesar. Milli-Q water (18.2 M Ω , filtered with filter pore size 0.22 μ M) was from Millipore. All solvents used were of analytical grade and were purchased from Sigma-Aldrich. All chemicals were used as received. Briefly, in a 50 mL three neck round bottom flasks equipped with a water cooled-condensers connected to a standard Schlenk line, 0.353 g (1 mmol) of iron (III) acetylacetonate and 0.78 g (4.5 mmol) of decanoic acid were dissolved in 18 mL of dibenzyl ether (DBE) and 7 mL of squalane. After degassing for 120 minutes at 65 °C, the mixture was heated up to 200 °C (3 °C/min) and kept at this value for 2.5 h. Finally the temperature was increased (7 °C/min) up to 310 °C and maintained at this value for 1 h. After cooling down to room temperature, 60 mL of acetone were added and the solution was centrifuged at 8500 rpm. The collected black precipitate was dispersed in 2-3 mL of chloroform and the washing procedure was repeated for at least two more times. Finally the collected particles were dispersed in 15 mL of chloroform. For the water transfer, 15 mL of gallol-modified polyethylene glycol (GA-PEG, $M_w \approx 3$ kDa)⁴³ solution (0.1 M in chloroform containing 1 mL triethylamine), were added to a solution of the NPs in chloroform and stirred over night at room temperature. Then, 10 mL of de-ionized water were added resulting in the formation of two phases. After emulsification by means of shaking, the phases were allowed to separate and the aqueous phase containing the GA-PEG coated magnetic NPs was collected. This step was repeated until all NPs were transferred to water. The excess of GA-PEG was removed by dialysis over night at room temperature in de-ionized water bath using a cellulose membrane tubing (Molecular weight cut off (MWCO) of 50 kDa). This step was repeated 5 times. Finally, the aqueous solution containing the NPs was concentrated by centrifugation by using a centrifuge filter (MWCO of 100 kDa) to an iron concentration of about 15-16 g/L (as determined by Induced Coupled Plasma -Atomic Emission Spectroscopy, ICP-AES, Thermo Fisher).

Synthesis of capsules: Template microparticles of CaCO_3 were obtained by mixing aqueous solutions of CaCl_2 (5 mL, 0.33 M) and Na_2CO_3 (5 mL, 0.33 M) under magnetic stirring at room temperature.²⁰ Polyelectrolyte walls were assembled around the CaCO_3 template cores ($\sim 4.5 \mu\text{m}$ diameter, 10 mL, 165 mg) by LbL coating of alternating layers of poly(allylamine hydrochloride) (PAH, $M_w \approx 56$ kDa) as positive polyelectrolyte and poly(styrene sulfonate) (PSS, $M_w \approx 70$ kDa) as negative polyelectrolyte, using standard protocols reported in literature.⁵⁴ For the LbL assembly the CaCO_3 particles were mixed with 5 mL of 2 mg/mL polymer solutions made in Milli-Q water, with 0.5 M of NaCl. As 4th layer a stronger positively charged polymer, poly(acrylamide-co-diallyl-dimethylammonium chloride) (P(Am-DDA)), was assembled to the LbL wall. P(Am-DDA) improves the attachment of magnetic NPs.⁵⁵ In this regard, 1 mL of magnetic NP solution ($c(\text{Fe}) = 15.65$ g/L) was added to the capsule solution. The concentration of magnetic NPs within the capsule shell can be tailored but decreasing the concentration of this NP solution.⁵⁵ Magnetic NPs were attached to the capsule wall on the positive layer of P(Am-DDA) *via* their negative charge (zeta potential of the magnetic NPs $\zeta = -20.9 \pm 0.3$ mV) and further LbL coatings of alternating layers of PAH and PSS were added. The final architecture of the LbL wall was (PSS/PAH)(PSS/P(Am-DDA) NPs (PAH)(PSS/PAH)₂). After dissolution of the CaCO_3 core by adding 10 mL of an ethylenediamine-tetraacetic acid disodium (EDTA) solution (0.2 M, pH 7) the capsules were filled with Cascade Blue-labelled dextran (10 kDa) *via* post-loading and further temperature shrinking of the LbL wall at 65 °C for one hour.²⁰ For this purpose 2 mL of an aqueous solution of 1 mg/mL of Cascade Blue-labelled dextran were mixed for 30 minutes with a concentrated solution of capsules (2 mL). The calculated percentage of loading by determining the residual amount of non-encapsulated Blue-labelled dextran *via* UV-vis spectroscopy was around 60 %. The final concentration was $3.3 \cdot 10^8$ capsules/mL (in 5 mL) measured with a hemocytometer and 1.6 g/L of Fe content ($4.8 \cdot 10^{-12}$ g Fe/capsule). The packing fraction, defined as the total volume occupied by the nanocubes divided by the volume within the capsule shell in which the NPs are distributed is around 100%, as the nanocubes are bigger than the polymer part of shell. For the calculation we refer to the Supporting Information and Abbasi *et al.*⁵⁵ The capsules were characterized with optical microscopy, transmission electron microscopy (TEM), and dynamic light scattering (DLS) (*cf.* Fig. 1). The capsule diameter was obtained by analysing optical microscopy images with the software UTHSCSA Image Tool (version 3.0).

Cargo release *via* magnetothermal heating: For the magnetothermal heating experiments a commercially available set-up was used (DM100 Series, nanoScale Biomagnetics Corp.). Experiments were performed on a concentrated (three times) capsule solution with an iron content of 4.8 g/L ($9.9 \cdot 10^8$ capsules/mL; $4.8 \cdot 10^{-12}$ g Fe *per* capsule). For a more detailed explanation about the used iron concentration we refer to the Supporting Information. Before heating experiments, the capsule solution was purified from Cascade Blue-labelled dextran, which has leaked out the capsules. For this purpose 350 μL of capsule solution were placed on top of a magnet (0.2 T) for 20 minutes and the capsules were collected (due to the magnetic NPs in their walls) at the bottom, while the supernatant was discarded. Then 350 μL of fresh Milli-Q water was added to the precipitate, followed by careful shaking, in order to redisperse capsules in solution. In order to quantify the possible presence of free Cascade Blue-labelled dextran, after adding fresh Milli-Q water, the solution was again placed on top of a magnet for 20 minutes. After this the capsules were collected at the bottom, the supernatant was withdrawn, and its absorption spectrum recorded, which did not show significant leaching of Cascade Blue-labelled dextran. The sample was then split in two aliquots: 250 μL of test-sample to be treated and 100 μL control sample.

The test-sample was placed under an AMF (300 kHz, 24 kAm⁻¹) for 90 minutes and the temperature of the solution was monitored (*cf.* Fig. 2). The control sample was kept at room temperature for 90 minutes. Both samples were then placed again on a magnet for 20 minutes to collect the capsules. Then supernatants were collected and filtered by using Microcentrifuge Spin Cups and Columns (MWCO cut-off 100 kDa), in order to remove capsule fragments from the supernatant, which may not have precipitated. Absorption and fluorescence emission spectra of the supernatants were recorded using quartz cuvettes (*cf.* Fig. 3). In addition TEM images of the precipitate containing the capsules were recorded (*cf.* the Supporting Information).

Results and Discussion

Capsules of $4.6 \pm 0.4 \mu\text{m}$ diameter with a zeta potential of $\zeta = +12.05 \pm 0.5 \text{ mV}$ and decorated with iron oxide nanocubes were successfully synthesized using an LbL approach (Fig. 1A). The presence of iron oxide nanocubes ($18 \pm 2 \text{ nm}$ NP diameter) accounts for the strong interaction of the capsules with a static magnetic field (after less than 5 minutes most of the sample was collected when placed under a magnet of 0.2 T). Despite the incorporation of the magnetic NPs at a high concentration, the geometry of the capsules was rather spherical. The presence of magnetic NPs and the loading of the capsules with Cascade Blue-labelled dextran were confirmed by TEM images and optical microscopy, respectively (*cf.* Fig. 1 and the Supporting Information).

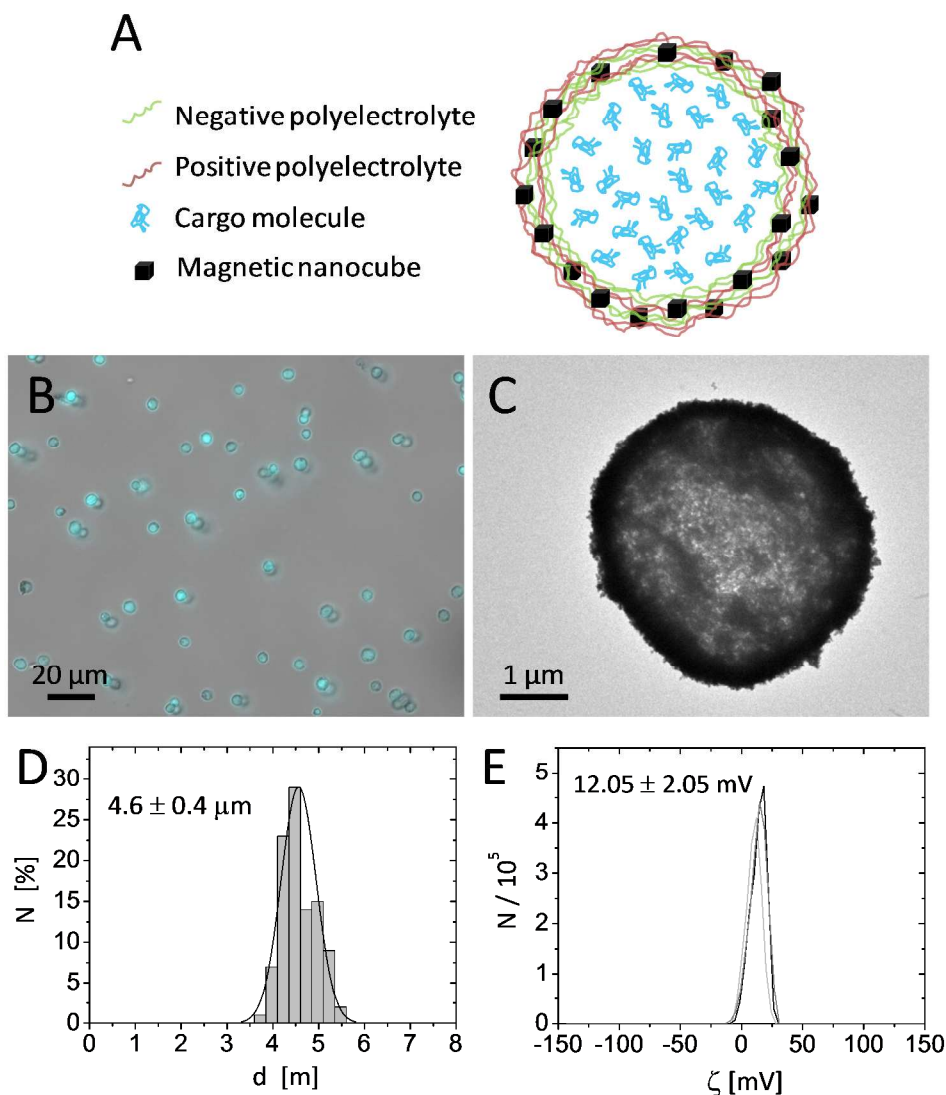


Fig. 1 A) Sketch of one polyelectrolyte capsule comprising Cascade Blue-labelled dextran as fluorescent cargo in the cavity and magnetic NPs in the wall. B) Optical microscopy image of capsules dispersed in water showing the bright field and blue fluorescence channel (excitation 365/50 nm, beam splitter 395 nm and emission 445/50 nm) corresponding to the emission of Cascade Blue-labelled dextran. The scale bar corresponds to 20 μm . C) TEM image of dried capsules. The scale bar corresponds to 1 μm . D) Histogram of the size distribution fitted with a Gaussian curve. E) ζ -potential measurements of the polyelectrolyte capsules in water. The values are the results of three independent measurements.

Because iron oxide nanocubes have shown very efficient heating performances,⁵¹ it should be possible to trigger the release of encapsulated Cascade Blue-labelled dextran by an AMF *via* thermal destruction of the capsule wall in which the nanoparticles are embedded. In order to demonstrate magnetothermal heating, a solution containing capsules with an iron concentration of 4.8 g/L was exposed to an AMF for 90 minutes. Upon exposure to the AMF, the used capsule concentration ensured a final temperature of about 90 °C in dynamic equilibrium (*cf.* Fig. 2). In fact, under the same experimental magnetic field conditions the finally reached temperature clearly did depend on the capsules (*i.e.* iron) concentration. Lower concentrations lead to lower final temperatures (*cf.* the Supporting Information). For instance, a capsule solution with a Fe content of 1.5 g/L raised the temperature only to 40 °C, whereas with a Fe

content of 2.8 g/L temperature could be raised to 62 °C. Thus control of capsules/iron concentration is of paramount importance, as the final temperature plays an important role on the opening of the capsules. It is worthy to underline that the final temperature will depend not only on the concentration of microcapsules, but also on their heating efficiency, which could be different with respect to “free” iron oxide nanocubes. In this regard, the specific absorption rate (SAR) was calculated from the temperature vs. time curves leading to a value of 427 W/g_{Fe} (at 300 kHz and 24 kAm⁻¹). This SAR value is below the value for “free” iron oxide nanocubes (824 W/g_{Fe} at 300 kHz and 24 kAm⁻¹).⁵¹ The lower performance can be explained as a result of a low thermal conductivity due the polymer coating as well as due to magnetic dipole-dipole interactions.^{56, 57} In addition it is worthy to underline that the SAR value decreases while decreasing the concentration of microcapsules in solution (*cf.* the Supporting Information).

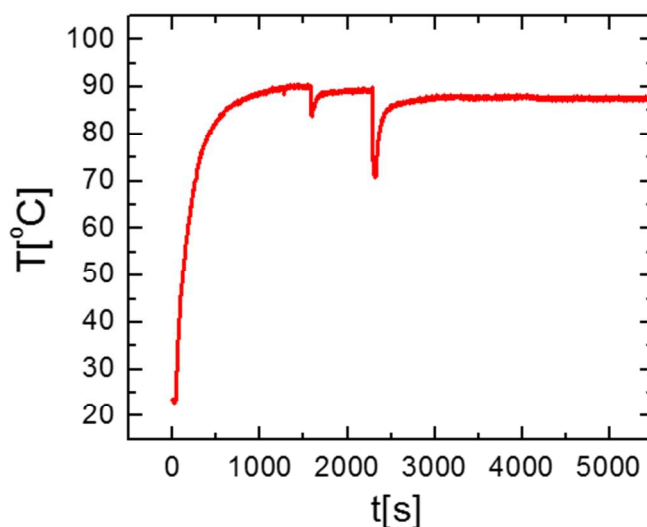


Fig. 2 Bulk temperature $T(t)$ as a function of time of a solution of capsules [4.8 g/L of Fe] placed under an AMF (300 kHz and 24 kAm⁻¹) for 90 minutes. During the experiment the solution was removed from the cavity where the AMF was applied (dips in the curve at 1500 s and 2250 s) in order to control and shake the solution.

In order to evaluate the influence that the AMF had on the capsules, and hence the temperature increase, TEM images from aliquots of the solution with AMF exposed capsules and the control sample were compared (*cf.* the Supporting Information). In the AMF treated capsules some damage in form of partially broken walls could be observed, together with the presence of some free magnetic NPs which had been released from the capsule walls. Both effects could not be found in the control capsules. However, even if some evidences of the effect of AMF exposure were observed, these results are clearly purely qualitative and the observable difference between both samples is at best relatively small. We thus performed an additional study based on recording the absorption and fluorescence spectra of the supernatant, in order to probe release of Cascade Blue-labelled dextran from the capsules upon AMF exposure (*cf.* Fig. 3). Note that before experiments eventually leached dye had been removed and in an additional control no significant further leaching was observed on the time scale of experiments. For the control sample, after 90 minutes at room temperature (no AMF) a rather small enhancement in the absorption and fluorescence spectra was observed, which is likely ascribed to a slow leakage of Cascade

Blue-labelled dextran from the capsules (*cf.* Fig. 3). On the other hand, in the case of AMF exposure remarkable changes in the absorption and fluorescence signals of the supernatant were observed. The fluorescence peak was centred at 420 nm, corresponding to the spectral feature of the fluorescence signal of free Cascade Blue-labelled dextran. In absorption however, for the AMF exposed sample, there was a strong and broad signal with a peak at 270 nm, and the characteristic absorption peaks of the free Cascade Blue-labelled dextran were partially hidden under this signal. This signal was clearly not present in the spectra of the control sample and not in the initial supernatant. The absorption peak at 270 nm might be attributed to the presence of small polymeric fragments derived from the broken capsule walls, which show a strong absorption below 300 nm (*cf.* the Supporting Information). Indeed, this hypothesis is supported by the TEM images of AMF treated capsules in which a surface damage was observed. We thus conclude that, besides the release of Cascade Blue-labelled dextran as observed by the fluorescence spectra, the heat generated under an AMF by the magnetic NPs in the capsules walls might also partially damage the polymeric wall in a way that polymer fragments, which absorb in the UV region, are released. In this context, Lu et al. studied the change of permeability of polyelectrolyte capsules containing magnetic nanoparticles using frequencies from 100 to 1000 Hz, while keeping the strength of the magnetic field constant at 95.5 kAm^{-1} .⁴⁵ They observed that low frequency AMFs (150 Hz, 95.5 kAm^{-1} , 30 minutes) increased the permeability of the polyelectrolyte walls and the temperature up to $50 \text{ }^\circ\text{C}$. However, frequencies beyond 300 Hz did not increase the permeability even after 1 hour of irradiation. The change of permeability was associated to NP agitation at low frequency AMFs and temporal disturbance of the polyelectrolyte wall. The temperature effect in the permeability was dismissed after doing control experiments with capsules heated at $50 \text{ }^\circ\text{C}$. Contrary, in our experiments capsules released cargo molecule after irradiation with an AMF of 300 Hz and the disruption of the wall must be ascribed to the higher heat production ($90 \text{ }^\circ\text{C}$) due to the presence iron nanocubes and the rupture of the polymeric wall observed in TEM images.

Finally, the fluorescence intensities of the capsules before and after treatment of AMF irradiation were recorded with confocal microscopy. In a population of over 400 capsules an evident decrease of the mean fluorescence intensity was observed for the AMF treated capsules as compared to the control sample (*cf.* the Supporting Information). However, the AMF treatment did not release all the cargo molecules within the polyelectrolyte capsules, as it has also been observed in photothermal controlled release *in vitro*.²⁰ This is due to the structure of the polyelectrolyte capsules. Polyelectrolyte capsules made on CaCO_3 templates can be described as a gel-like matrix, as (due to the porosity of CaCO_3) polyelectrolytes permeate within the template during the LbL assembly and after the core dissolution a polyelectrolyte matrix is formed within the inner cavity of the capsules.⁵⁸ Some cargo molecules can stay attached to the charged polyelectrolytes of the matrix, even after disruption of the wall. The decrease of fluorescence upon AMF exposure measured with confocal microscopy is an additional indication of the release of Cascade Blue-labelled dextran to the environment.

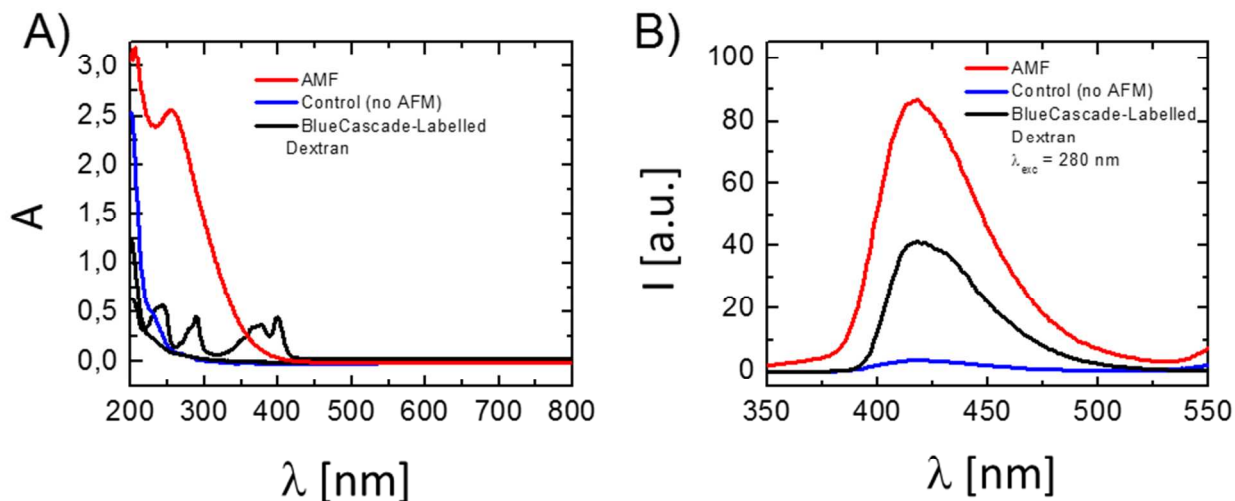


Fig. 3 A) UV-vis absorption spectra, and B) fluorescence emission spectra (at $\lambda_{\text{exc}} = 280$ nm excitation) of: i) free Cascade Blue-labelled dextran (black line), ii) the supernatant of a capsule solution which had been treated for 90 minutes under an AMF (300 kHz and 24 kAm^{-1}) (red line), and iii) the supernatant of a control sample of capsules which had been kept at room temperature for 90 minutes and thus had not been exposed to an no AMF (blue line).

Conclusions

The proof-of-concept experiment shown in this study suggests that release of molecular cargo from polyelectrolyte capsules by NP-mediated heating is not only possible by light-irradiation of plasmonic NPs, but also by AMF-irradiation of magnetic NPs. Owing the high heating performance of iron oxide nanocubes, damages in the polymer wall were prompted through an AMF, which allowed for release of the encapsulated molecular cargo. For successful remotely controlled release of cargo by magnetothermal heating the content of magnetic NPs has to be carefully tuned. In our case iron concentrations above 2.7 g/L (4.8 g/L) allowed for a suitable temperature increase for opening the wall of the capsules. In comparison to optical excitation, AMF excitation is barely absorbed by tissues, which should allow for convenient externally triggered release. This issue opens new and exciting possibilities of cargo release for *in vivo* applications, though the geometry of the capsules would need to be optimized towards such applications. In this regard, the future direction of this research should deal with the requirement of *in vivo* applications which preferentially will involve smaller capsules that can be fabricated using the LbL technique.^{59,60}

Acknowledgements

The authors are grateful to Dr. Pablo del Pino and Prof. Heinz Jänsch for helpful discussions, and to Simone Nitti and Giammarino Pugliese for helping with sample preparation. This work was supported by HSFP (project RGP0052/2012 to WJP), by the European project Magnifyco (Contract NMP4-SL-2009-

228622 to TP) and by the Italian AIRC project (contract n. 14527 to TP). X.Y. acknowledges support by the Chinese government (CSC, Nr. 2010691036).

References

1. P. Rivera_Gil, S. D. Koker, B. G. De_Geest and W. J. Parak, *Nano Letters*, 2009, 9, 4398-4402.
2. S. De Koker, B. G. De Geest, C. Cuvelier, L. Ferdinande, W. Deckers, W. E. Hennink, S. De Smedt and N. Mertens, *Advanced Functional Materials*, 2007, 17, 3754-3763.
3. H. Shen, H. Shi, M. Xie, K. Ma, B. Li, S. Shen, X. Wang and Y. Jin, *J. Mater. Chem. B*, 2013, 1, 3906-3917.
4. A. Johnston, G. Such and F. Caruso, *Angewandte Chemie International Edition*, 2010, 49, 2664.
5. M. Ochs, S. Carregal-Romero, J. Rejman, K. Braeckmans, S. C. De Smedt and W. J. Parak, *Angewandte Chemie International Edition*, 2013, 52, 695-699
6. G. B. Sukhorukov, A. L. Rogach, B. Zebli, T. Liedl, A. G. Skirtach, K. Köhler, A. A. Antipov, N. Gaponik, A. S. Susha, M. Winterhalter and W. J. Parak, *Small*, 2005, 1, 194-200.
7. F. Caruso, *Chemistry-A European Journal*, 2000, 6, 413-419.
8. W. Tong, X. Song and C. Gao, *Chemical Society Reviews*, 2012, 41, 6103-6124.
9. Y. Yan, M. Bjornmalm and F. Caruso, *Chemistry of Materials*, 2014, 26, 452-460.
10. A. Sexton, P. G. Whitney, S.-F. Chong, A. N. Zelikin, A. P. R. Johnston, R. De Rose, A. G. Brooks, F. Caruso and S. J. Kent, *ACS Nano*, 2009, 3, 3391.
11. S. De Koker, T. Naessens, B. G. De Geest, P. Bogaert, J. Demeester, S. De Smedt and J. Grooten, *Journal of Immunology*, 2010, 184, 203-211.
12. G. B. Sukhorukov, A. A. Antipov, A. Voigt, E. Donath and H. Mohwald, *Macromolecular Rapid Communications*, 2001, 22, 44-46.
13. K. Liang, G. K. Such, Z. Zhu, S. J. Dodds, A. P. R. Johnston, J. Cui, H. Ejima and F. Caruso, *ACS Nano*, 2012, 6, 10186-10194.
14. A. M. Pavlov, V. Saez, A. Cobley, J. Graves, G. B. Sukhorukov and T. J. Mason, *Soft Matter*, 2011, 7, 4341-4347.
15. L. L. del Mercato, E. Gonzalez, A. Z. Abbasi, W. J. Parak and V. Puntès, *Journal of Materials Chemistry*, 2011, 21, 11468-11471.
16. B. Radt, T. A. Smith and F. Caruso, *Advanced Materials*, 2004, 16, 2184-2189.
17. A. S. Angelatos, B. Radt and F. Caruso, *J. Phys. Chem. B*, 2005, 109, 3071-3076.
18. A. G. Skirtach, A. M. Javier, O. Kreft, K. Köhler, A. P. Alberola, H. Möhwald, W. J. Parak and G. B. Sukhorukov, *Angew. Chem. Int. Ed.*, 2006, 45, 4612-4617.
19. A. Muñoz Javier, P. del Pino, M. F. Bedard, A. G. Skirtach, D. Ho, G. B. Sukhorukov, C. Plank and W. J. Parak, *Langmuir*, 2008, 24, 12517-12520.
20. S. Carregal-Romero, M. Ochs, P. Rivera Gil, C. Ganas, A. M. Pavlov, G. B. Sukhorukov and W. J. Parak, *Journal of Controlled Release* 2012, 159, 120-127.
21. G. Baffou and R. Quidant, *Laser & Photonics Reviews*, 2013, 7, 171-187.
22. X. Huang, P. Jain, I. El-Sayed and M. El-Sayed, *Lasers in Medical Science*, 2007, 23, 217-228.
23. S. Lal, S. E. Clare and N. J. Halas, *Acc Chem Res*, 2008, 41, 1842-1851.
24. D. P. O'Neal, L. R. Hirsch, N. J. Halas, J. D. Payne and J. L. West, *Cancer Letters*, 2004, 209, 171-176.
25. X. Huang, I. H. El-Sayed, W. Qian and M. A. El-Sayed, *J Am Chem Soc*, 2006, 128, 2115-2120.
26. L. R. Hirsch, R. J. Stafford, J. A. Bankson, S. R. Sershen, B. Rivera, R. E. Price, J. D. Hazle, N. J. Halas and J. L. West, *Proceedings of the National Academy of Sciences of the United States of America*, 2003, 100, 13549-13554.

27. D. Hühn, A. Govorov, P. Rivera Gil and W. J. Parak, *Advanced Functional Materials*, 2012, 22, 294-303.
28. S. Peeters, M. Kitz, S. Preisser, A. Wetterwald, B. Rothen-Rutishauser, G. N. Thalmann, C. Brandenberger, A. Bailey and M. Frenz, *Biomedical Optics Express*, 2012, 3, 435-446.
29. Z. Krpetic, P. Nativo, V. See, I. A. Prior, M. Brust and M. Volk, *Nano Letters*, 2010, 10, 4549-4554.
30. A. Topete, M. Alatorre-Meda, E. M. Villar-Alvarez, S. Carregal-Romero, S. Barbosa, W. J. Parak, P. Taboada and V. Mosquera, *Adv. Healthcare Mat.*, 2014, DOI: 10.1002/adhm.201400023.
31. S. J. Leung and M. Romanowski, *ACS Nano*, 2012, 6, 9383-9391.
32. R. Weissleder, *Nature Biotechnology*, 2001, 19, 316-317.
33. A. Vogel and V. Venugopalan, *Chem Rev*, 2003, 103, 577-644.
34. A. Jordan, R. Scholz, P. Wust, H. Fahling and R. Felix, *Journal of Magnetism and Magnetic Materials*, 1999, 201, 413-419.
35. Q. A. Pankhurst, J. Connolly, S. K. Jones and J. Dobson, *Journal of Physics D: Applied Physics*, 2003, 36, R167-R181.
36. H. Huang, S. Delikanli, H. Zeng, D. M. Ferkey and A. Pralle, *Nature Nanotechnology*, 2010, 5, 602-606.
37. M. Colombo, S. Carregal-Romero, M. F. Casula, L. Gutiérrez, M. P. Morales, I. B. Böhm, J. T. Heverhagen, D. Prospero and W. J. Parak, *Chemical Society Reviews*, 2012, 41, 4306-4334.
38. R. E. Rosensweig, *J. Magn. Magn. Mater.*, 2002, 252, 370-374.
39. R. Hiergeist, W. Andrä, N. Buske, R. Hergt, I. Hilger, U. Richter and W. Kaiser, *Journal of Magnetism and Magnetic Materials*, 1999, 201, 420-422.
40. R. Hergt, S. Dutz, R. Mueller and M. Zeisberger, *Journal of Physics - Condensed Matter*, 2006, 18, S2919-S2934.
41. Q. A. Pankhurst, N. K. T. Thanh, S. K. Jones and J. Dobson, *Journal of Physics D - Applied Physics*, 2009, 42, 224001/224001-224001/224015.
42. J. P. Fortin, C. Wilhelm, J. Servais, C. Menager, J. C. Bacri and F. Gazeau, *J. Am. Chem. Soc.*, 2007, 129, 2628-2635.
43. A. Riedinger, P. Guardia, A. Curcio, M. A. Garcia, R. Cingolani, L. Manna and T. Pellegrino, *Nano Letters*, 2013, 13, 2399-2406.
44. T. T. T. N'Guyen, H. T. T. Duong, J. Basuki, V. Montembault, S. Pascual, C. Guibert, J. Fresnais, C. Boyer, M. R. Whittaker, T. P. Davis and L. Fontaine, *Angewandte Chemie, International Edition*, 2013, 52, 14152-14156.
45. Z. H. Lu, M. D. Prouty, Z. H. Guo, V. O. Golub, C. Kumar and Y. M. Lvov, *Langmuir*, 2005, 21, 2042-2050.
46. S.-H. Hu, C.-H. Tsai, C.-F. Liao, D.-M. Liu and S.-Y. Chen, *Langmuir*, 2008, 24, 11811-11818.
47. N. L. Klyachko, M. Sokolsky-Papkov, N. Pothayee, M. V. Efremova, D. A. Gulin, N. Pothayee, A. A. Kuznetsov, A. G. Majouga, J. S. Riffle, Y. I. Golovin and A. V. Kabanov, *Angew. Chem., Int. Ed.*, 2012, 51, 12016-12019.
48. R. Hergt and S. Dutz, *Journal of Magnetism and Magnetic Materials*, 2007, 311, 187-192.
49. J. H. Lee, J. T. Jang, J. S. Choi, S. H. Moon, S. H. Noh, J. W. Kim, J. G. Kim, I. S. Kim, K. I. Park and J. Cheon, *Nature Nanotechnology*, 2011, 6, 418-422.
50. P. Guardia, R. Di Corato, L. Lartigue, C. Wilhelm, A. Espinosa, M. Garcia-Hernandez, F. Gazeau, L. Manna and T. Pellegrino, *Acs Nano*, 2012, 6, 3080-3091.
51. P. Guardia, A. Riedinger, S. Nitti, G. Pugliese, S. Marras, A. Genovese, L. Manna and T. Pellegrino, 2014, DOI: 10.1039/C4TB00061G.
52. K. Katagiri, Y. Imai, K. Koumoto, T. Kaiden, K. Kono and S. Aoshima, *Small*, 2011, 7, 1683-1689.
53. K. Katagiri, M. Nakamura and K. Koumoto, *Acs Applied Materials & Interfaces*, 2010, 2, 768-773.

54. L. L. del Mercato, A. Z. Abbasi and W. J. Parak, *Small*, 2011, 7, 351-363.
55. A. Z. Abbasi, L. Gutierrez, L. L. del Mercato, F. Herranz, O. Chubykalo-Fesenko, S. Veintemillas-Verdaguer, W. J. Parak, M. P. Morales, J. M. Gonzalez, A. Hernando and P. de la Presa, *J. Phys. Chem. C*, 2011, 115, 6257-6264.
56. C. Haase and U. Nowak, *Phys. Rev. B*, 2012, 85, 045435.
57. C. Martinez-Boubeta, K. Simeonidis, D. Serantes, I. Conde-Leborán, I. Kazakis, G. Stefanou, L. Peña, R. Galceran, L. Balcells, C. Monty, D. Baldomir, M. Mitrakas and M. Angelakeris, *Adv. Funct. Mater.*, 2012, 22, 3737-3744.
58. D. V. Volodkin, A. I. Petrov, M. Prevot and G. B. Sukhorukov, *Langmuir*, 2004, 20, 3398-3406.
59. J. Schwiertz, W. Meyer-Zaika, L. Ruiz-Gonzalez, J. M. Gonzalez-Calbet, M. Vallet-Regi and M. Epple, *Journal Of Materials Chemistry*, 2008, 18, 3831-3834.
60. S. Krol, S. del Guerra, M. Grupillo, A. Diaspro, A. Gliozzi and P. Marchetti, *Nano Letters*, 2006, 6, 1933-1939.